ELSEVIER

Marine Geology 224 (2005) 1–22

MARINE GEOLOGY
INTERNATIONAL JOURNAL OF MARINE GEOLOGY, GEOCHEMISTRY AND GEOPHYSICS

www.elsevier.com/locate/margeo

Geology and tsunamigenic potential of submarine landslides in Santa Barbara Channel, Southern California

Michael A. Fisher [a,*], William R. Normark [a], H. Gary Greene [b], Homa J. Lee [a], Ray W. Sliter [a]

[a] *U.S. Geological Survey, MS 999, 345 Middlefield Road, Menlo Park, CA 94025, United States*
[b] *Moss Landing Marine Laboratory, 8272 Moss Landing Road, Moss Landing CA 95039, United States*

Received 25 June 2004; received in revised form 7 July 2005; accepted 21 July 2005

Abstract

A large submarine landslide complex and four small landslides developed under the Santa Barbara Channel, suggesting a potential hazard from landslide-generated tsunamis. We integrate offshore stratigraphy and geologic structure, multibeam bathymetric information, and several kinds of seismic-reflection data to understand how and when the submarine landslides formed. Seismic-reflection data show that mass failure along the slope began at least 200 ka ago. Landslides appear as zones of poor reflectivity having an irregular upper surface, and these zones alternate vertically with strong parallel reflections. The emplacement ages of two of the three main landslide lobes are well established at 8 and 10 ka. The source material for the youngest part of the landslide complex was sediment of probable late Pleistocene and Holocene age that accumulated in a shelf-edge delta. Directly under this delta, growth of faults and anticlines was particularly intense and tended to oversteepen the deltaic deposits. These active structures also formed migration pathways and reservoirs for aqueous and hydrocarbon fluids from the deep basin. Tsunami deposits have been described from a low-lying area near Santa Barbara, and numerical modeling of tsunamis generated by hypothetical landslides in Santa Barbara Channel indicates a moderate to severe threat [Borrero, J.C., Dolan, J.F. and Synolakis, C.E., 2001. Tsunamis within the eastern Santa Barbara Channel. Geophys. Res. Lett., 28(4): 643–646.], involving wave runups of 2–20 m, for a range of assumed landslide volumes. Inundation from these waves, however, is expected to be highly focused so that only narrow (~10-km) sections of the shoreline would be affected.

Keywords: mass wasting; landslide; tsunami; structural controls

1. Introduction

The Santa Barbara Channel separates the southern California mainland from the east–west island chain between Anacapa and San Miguel Islands (Fig. 1). The channel's north shore faces a relentless increase

* Corresponding author. Tel.: +1 650 329 5158.
E-mail address: mfisher@usgs.gov (M.A. Fisher).

0025-3227/$ - see front matter.
doi:10.1016/j.margeo.2005.07.012

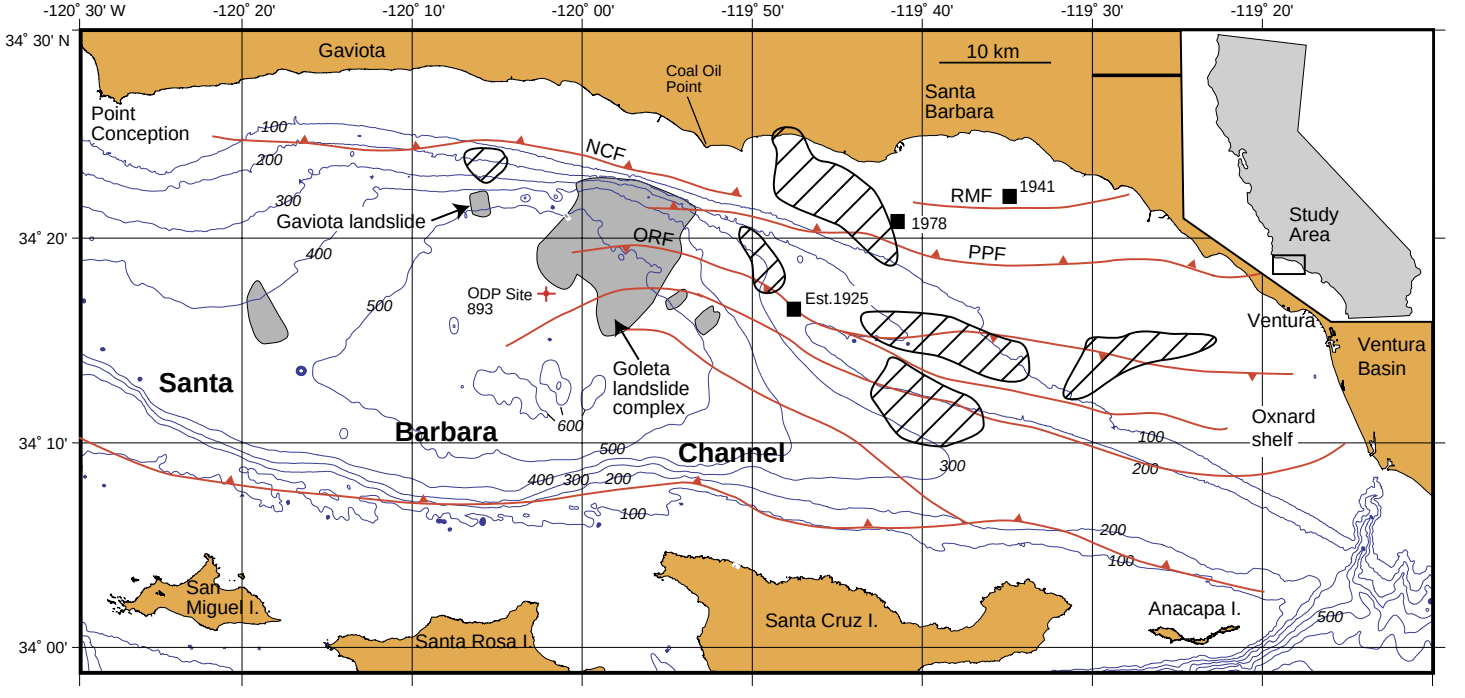

Fig. 1. Map of the western Santa Barbara Channel, where submarine landslides (gray shaded areas) are mostly dislodged from the north side. Major faults (red lines) include the Pitas Point (PPF), the Red Mountain (RMF), the North Channel (NCF), and the Oak Ridge (ORF). Black squares show some of the main earthquakes that struck the study area. Cross-hatched areas are clusters of seismicity, some of which concentrate along known fault trends.

in population, and people there must deal with geologic hazards such as large earthquakes and tsunamis caused by local earthquakes and by submarine landslides. Ultimately, these hazards stem from the numerous large faults that cleave the deep sedimentary basin under the Santa Barbara Channel (Fig. 1). In the western part of this channel, the large Goleta submarine landslide complex developed along one of the major faults, and other subsidiary landslides formed recently (Figs. 1 and 2), suggesting a potential hazard from landslide-generated tsunamis.

Here we discuss the mechanisms of generation and emplacement of the submarine landslides in the Santa Barbara Channel and whether they might cause tsunamis. Particular questions include: What factors caused the main landslides to be concentrated along one short segment of the continental shelf edge (Figs. 1 and 2)? How old are the landslides, what triggered them, and are tsunamis from future landslides a hazard to be reckoned with?

2. The Santa Barbara Basin

2.1. Regional setting and tectonic development

The sedimentary basin under the Santa Barbara Channel is the submerged westward extension of the onshore Ventura basin. Together these basins form part of the east–west Transverse Ranges province that cuts at a high angle across the regional, northwest grain of major faults and mountain ranges elsewhere in southern California. The south boundary of the Santa Barbara Basin is marked by the northern Channel Islands, extending from Anacapa to San Miguel (Fig. 1).

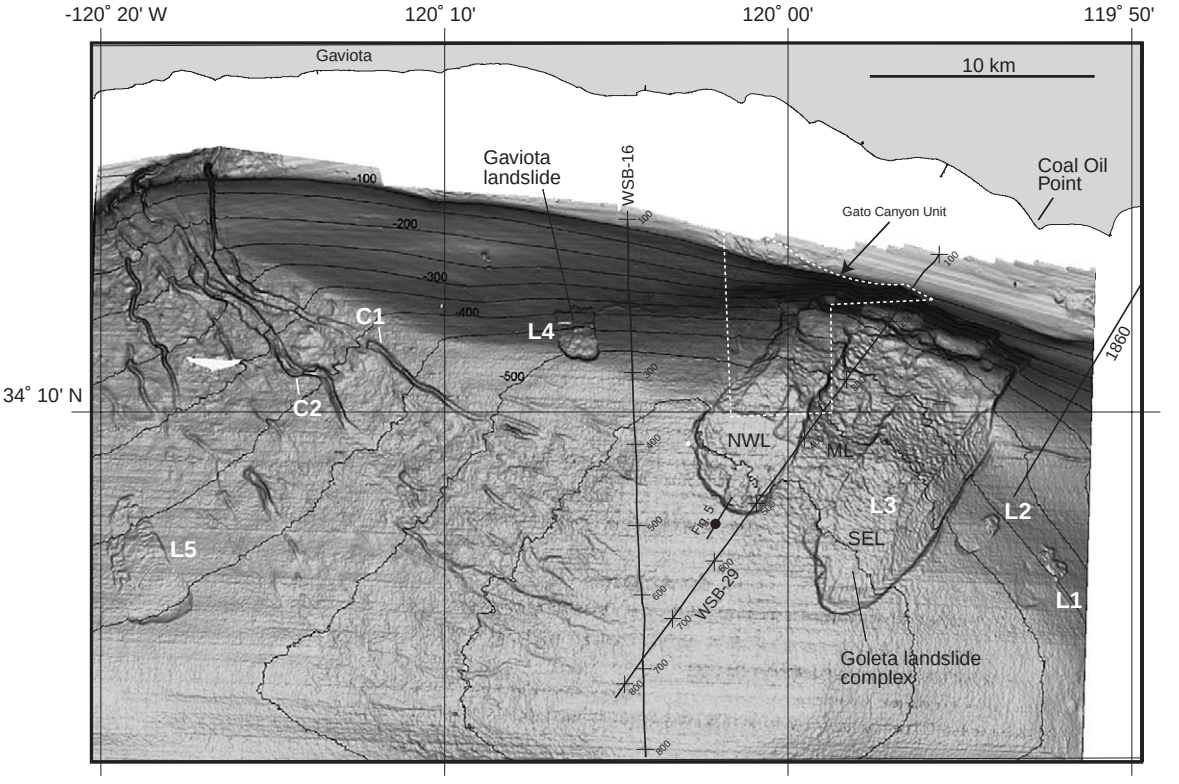

Fig. 2. Multibeam bathymetric data collected by Monterey Bay Aquarium Research Institute (MBARI). Seafloor data shown as shaded-relief of topographic slope. Black dot is ODP Site 893. Landslides are denoted by the letter "L" with a number: L3 is the Goleta landslide complex, and L4 is the Gaviota mudslide. The Goleta landslide complex includes three main surficial lobes: NWL is northwest lobe; ML is middle lobe; SEL is southeast lobe. Seafloor channels are indicated with the letter "C" and a number.

The Ventura basin contains one of the world's thickest sections (6 km) of Pliocene and Quaternary rocks (Yeats et al., 1994; Sylvester and Brown, 1997), attesting to the high intensity of basin-forming tectonics. In general, this intensity decreased westward from the Ventura Basin toward the study area in western Santa Barbara Channel. Moreover, large onshore faults—like the Oak Ridge, the Pitas Point and the Red Mountain—extend westward from the Ventura Basin, and some extend as far west as the study area (Fig. 1).

Before the Miocene, the tectonic regime of the area now occupied by the Santa Barbara Basin evolved above the east-subducting Farallon oceanic plate (Atwater, 1970; Engebretson et al., 1985; Nicholson et al., 1994). Early Miocene and older rocks were accreted within the subduction zone or deposited on top of the accretionary wedge in a series of north-trending forearc basins. Subduction ceased during the early Miocene, when a remnant piece of the Farallon plate began to move northward with the Pacific plate (Nicholson et al., 1994). During this tectonic transition, regional oblique rifting and strike-slip deformation replaced margin-normal compression. The resulting oblique extension is thought to have been caused by the large-scale (~90°) clockwise rotation of the western Transverse Ranges into their present east–west orientation (Kamerling and Luyendyk, 1985; Hornafius et al., 1986). Since the late Pliocene, about 5 Ma ago, the Santa Barbara Basin has been subjected to strong north–south compression, as the San Andreas fault became the active plate boundary and the Gulf of California opened.

2.2. Correlating Miocene and younger stratigraphy using seismic-reflection data

Tennyson and Kropp (1998) correlated deep-penetration seismic-reflection data with stratigraphic data from offshore oil wells in the western Santa Barbara Basin. Using this correlation, we traced distinctive, basin-wide reflections to show the age of rocks near the Goleta landslide (Table 1; Fig. 3). Reflections from within the middle and late Miocene Monterey and late Miocene and Pliocene Sisquoc Formations are continuous over long distances, whereas reflections from rocks in the overlying Pico Formation and Quaternary deposits are discontinuous and vary considerably in amplitude. This appearance change coincides with the increasing proportion of terrigenous material supplied to the basin. Another continuous reflection is from within the late Quaternary section (reflection C in Fig. 3).

Table 1
Approximate ages of reflective horizons

Reflection	Age*
A	170 ka
B	200 ka
C	350 ka
D	Base late Pliocene rocks (base of Pico Formation, top of Sisquoc Formation)
E	Base late Miocene rocks (base Sisquoc Formation, top of Monterey Formation)

*Numerical ages are estimated by extrapolating age dates obtained from ODP Site 893 (Fig. 4). Non-numerical dates come from correlating seismic-reflection data to stratigraphic information in Tennyson and Kropp (1998).

Late Quaternary sediment in Santa Barbara Basin is known from drilling results obtained at ODP Site 893, which is located about 1 km southwest of the toe of the Goleta landslide complex (Fig. 2). This drilling provides a detailed chronostratigraphy and oxygen-isotope record for the shallow sediment (Kennett, 1995; Ingram and Kennett, 1995; Behl and Kennett, 1996). Sediment from Site 893 yielded reservoir-corrected C14 ages, from planktic foraminifera, as old as 40 ka at a depth of about 68 m in the hole. To derive age estimates for deeper sediment, Kennett (1995) extended dates back to 164 ka by comparing drilling data to the SPECMAP global marine oxygen-isotope curve (Martinson et al., 1987).We correlated ODP-drilling results with high-resolution seismic-reflection data, using sediment velocities from Elliott and Kamerling (1995) to convert depth in the ODP drill hole to two-way travel time. The two seismic sections in Fig. 4 were obtained with Huntec and minisparker seismic sources and show the varied seismic–stratigraphic expression of the late Quaternary section near the ODP site and landslide toe.

2.3. Basin structure

During the past 4–5 Ma, the Santa Barbara Basin has undergone strong north–south compression (e.g. Yeats et al., 1988; Yeats and Huftile, 1995; Sylvester

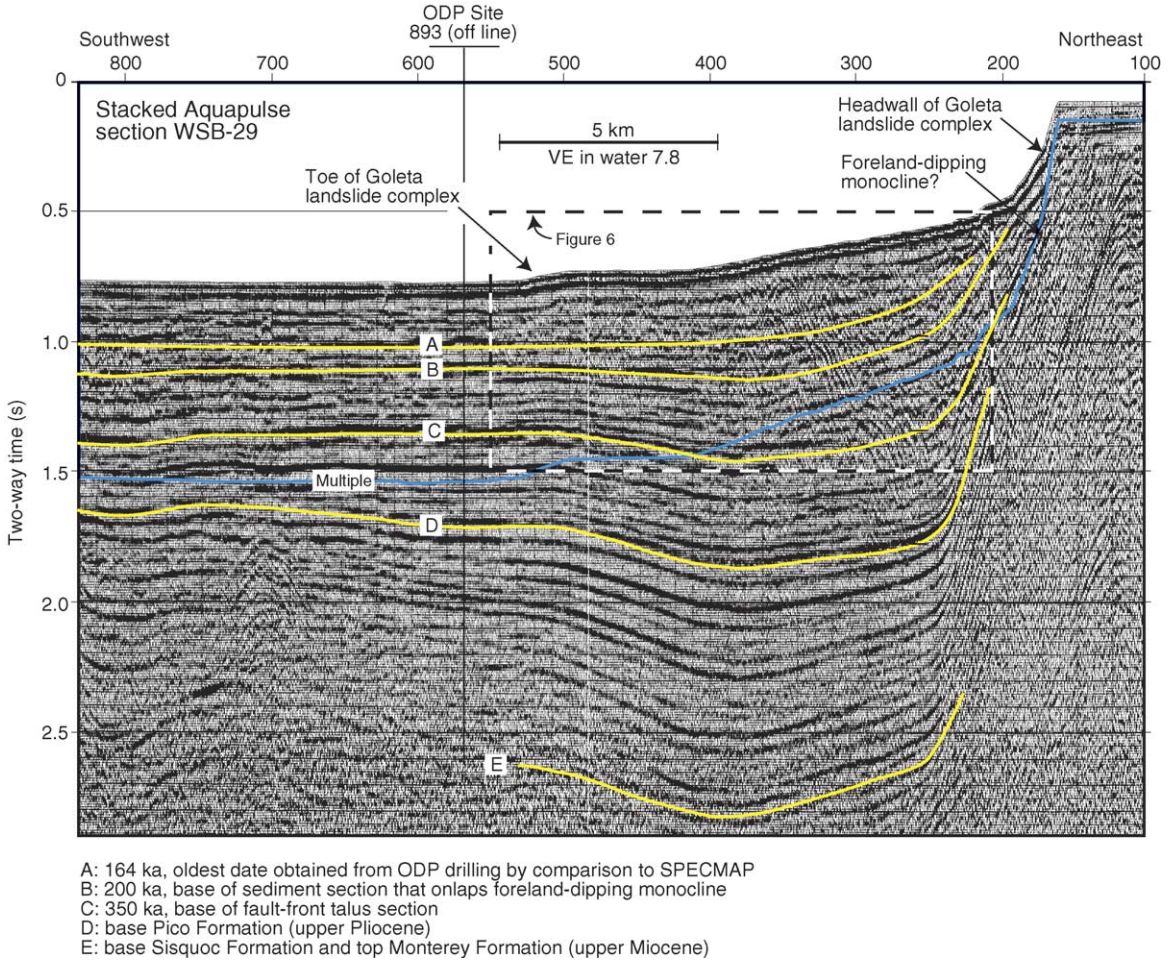

Fig. 3. Aquapulse seismic-reflection data across the Goleta landslide complex. Location shown in Fig. 2. Approximate dates of seismic horizons (Table 2) are from extrapolation of the biostratigraphy at ODP Site 893 and from correlation through seismic data of results in Tennyson and Kropp (1998).

and Brown, 1997; Sorlien et al., 2000). Presently active faults show mainly high-angle reverse or left-lateral oblique-slip movement. Sorlien et al. (2000) measured the rate of crustal shortening by faulting and folding across the eastern Santa Barbara Channel and found that the highest shortening rates occurred after about 1 Ma ago.

The structural configuration of the deep Santa Barbara Basin is shown by contours on a stratigraphic horizon near the top of the middle and late Miocene Monterey Formation (Heck, 1998) (Fig. 5), probably a horizon near reflection E on Fig. 3. We explain below the importance of this deep structure to the analysis of shallow landslides, which stems mainly from the close correspondence in location of landslides and deep anticlines (Fig. 5).

The map of deep structure (Fig. 5) also shows the locations of offshore faults that underlie the area near the Goleta landslide complex. According to Heck (1998) (Fig. 5), near the headwall of the landslide complex, the Pitas Point and North Channel Faults approximately follow the shelf edge, and the faults are discontinuous (Fig. 5). Consequently, the headwall of the slide complex may be underlain by the complicated structure of a displacement transfer zone. Other researchers (Sorlien and Kamerling, 2000; Sorlien et al., 2000; Kamerling et al., 2001, 2003) proposed that these faults, together with the Red Mountain fault, are

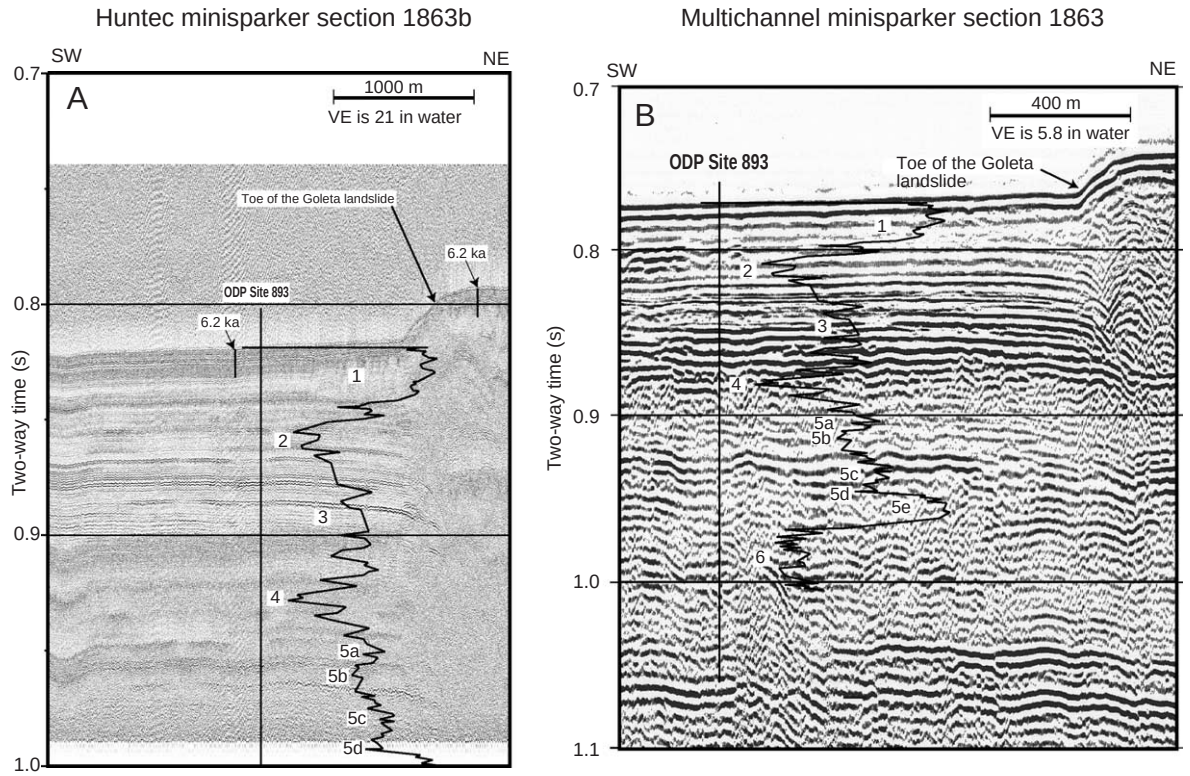

Fig. 4. (A) Very high resolution Huntec minisparker data over the ODP drill site 893 and the toe of the Goleta landslide complex. Section location is shown in Fig. 2. The irregular black curve shows the oxygen-isotope variation within drilled sediment (Kennett, 1995). The numbers in white boxes indicate isotope stages. (B) High resolution minisparker data over the ODP drill site and the toe of the landslide. Section location is shown in Fig. 2.

splays of the North Channel–Pitas Point–Red Mountain fault system, which in aggregate extends more than 60 km east–west. The fault system dips 40–50° north, and continues to depths as great as 18–20 km. Numerous fault splays make up the overall fault system, and the splays accommodate local shortening, mainly by folding, in the footwall of the main Red Mountain fault. Clearly, the Goleta landslide complex is spatially associated with a major active fault system. West of the landslide complex, near the Hondo anticline (Fig. 5), movement along the fault system apparently began during the late Pliocene, and the fault has deformed rocks by transporting them southward over a deep-seated, north-dipping thrust fault (McGroder et al., 1994).

Sorlien et al. (2000) proposed that the offshore Oak Ridge fault is a significant south-dipping reverse fault, which accords with other research (e.g. Huftile and Yeats, 1995; Kamerling and Nicholson, 1996). In a contrary view, this fault has been interpreted to be an active kink band caused by southward movement of basin and basement rocks over an inflection in the deep-seated (10 km) inferred Channel Islands thrust fault (Shaw et al., 1994). This deep thrust fault could unleash an M ~7 earthquake.

3. Seismicity and locally generated tsunamis

Strong earthquakes near the Santa Barbara Channel represent a continuation of the highly active tectonism that has characterized this region during the late Cenozoic. Three major damaging earthquakes—during 1812, 1925, and 1978 (Fig. 1)—have struck the region of this study (Ellsworth, 1990). A seismograph was first installed around Santa Barbara in 1927, following

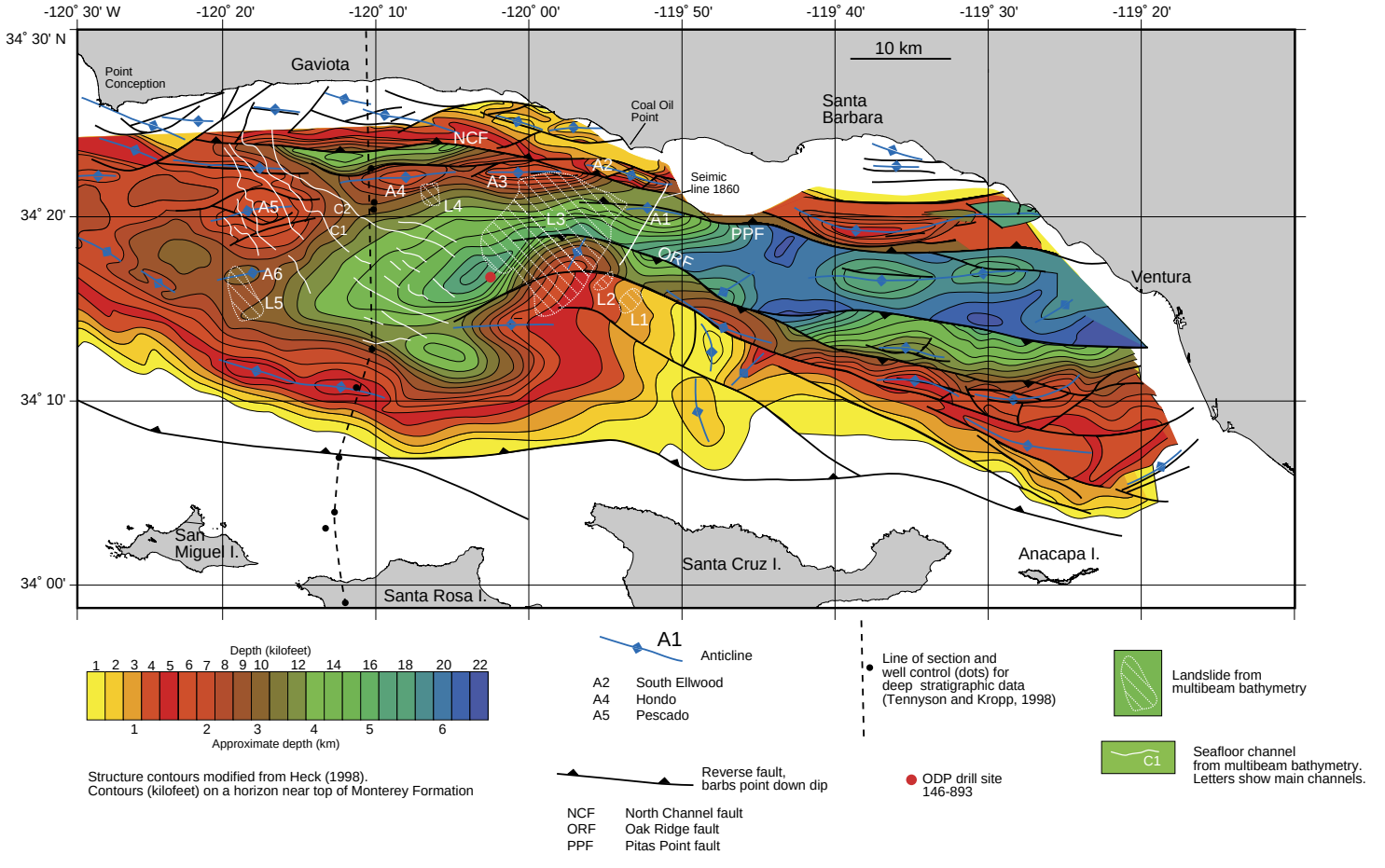

Fig. 5. Geologic structure of the Santa Barbara Basin shown by contours on a horizon near the top of the Monterey Formation (Heck, 1998). Submarine landslides, annotated with an "L" and a number, and anticlines, shown with an "A" and a number, share a close spatial association. Below the Goleta landslide complex (L3), the Oak Ridge Fault (ORF) curves southwest and dies out. The Pitas Point and North Channel Faults are shown as discontinuous (Heck, 1998), but they may be one fault (Sorlien et al., 2000).

the major earthquake in 1925, so earthquakes that occurred before then are known only from scant, primarily anecdotal information. The largest earthquake occurred in December 1812 and is thought to have been located somewhere within the Western Transverse Ranges or northern Santa Barbara Channel. This earthquake had a magnitude of ~7, and is regarded as one of the larger earthquakes in California history (Toppozada et al., 1981; Evernden and Thompson, 1985; Ellsworth, 1990). The 1812 earthquake reportedly caused a local tsunami with a run-up height of about 2 m (NOAA, 2003), although this possibility has been disputed (Grauzinis et al., 1965). Persistent reports of a small tsunami associated with the 1812 earthquake are the primary basis for its traditional location below the Santa Barbara Channel (Toppozada et al., 1981; Ellsworth, 1990). The 1925 earthquake had a magnitude of ~6.3 and was located just west of the City of Santa Barbara.

Most well located earthquakes occurred in the eastern half of the Santa Barbara Channel (Fig. 1). Earthquakes tend to cluster along known fault trends, like the Oak Ridge Fault and the North Channel–Pitas Point–Red Mountain fault system (Kamerling et al., 2001) (Fig. 1). A notable earthquake during 1978 (M_w=5.9) struck southwest of the city of Santa Barbara, at a depth of about 12 km. This quake may have occurred along a north-dipping thrust fault (Corbett and Johnson, 1982); however, a steeply dipping fault plane cannot be excluded (Yeats and Olson, 1984). During this earthquake, the rupture propagated northwestward from the offshore epicenter toward inhabited onshore areas (Lee et al., 1978).

Other reports of locally generated tsunamis include a small wave in 1854 that followed a moderate earthquake and the tsunami generated by the 1927 Lompoc earthquake located west of Point Conception (Satake and Somerville, 1992).

3.1. Previous findings about the submarine landslides

Submarine landslides in the Santa Barbara Basin, first described by Duncan et al. (1971), were analyzed in detail in support of proposed Federal petroleum lease sales (Richmond et al., 1981; Burdick and Richmond, 1982). The largest and most conspicuous slope failure is the Goleta slide southwest of Coal Oil Point (Varnes, 1978; Thornton, 1984, 1986; Edwards et al., 1995; Eichhubl et al., 2002) (Fig. 2). The Goleta landslide resulted from multiple mass wasting events. It consists of three main lobes—the northeast, middle, and southwest (Fig. 2)—that are composed of mud or debris flows. Slope sediment of probable late Quaternary age failed sequentially, causing the headwall to retreat northward. The seafloor over the slide lobes is relatively smooth over the toe sections, hummocky over the middle parts of the lobes, and irregular near the headwall. This distribution of morphologic features generally follows the morphologic subdivisions in Prior et al. (1984).

The Goleta landslide complex is 14 km long and 11 km wide, and its headwall scarp forms the shelf break at 100 m water depth. Three lobes of the landslide complex extend southwestward across the continental slope, reaching a maximum water depth of 570 m, but the lobes do not reach the basin plain. Locally, the headwall scarp is inclined at 40–45°. The seafloor just below the headwall scarp slopes at 27°, and near the toe, the seafloor inclination flattens to 1.5°. From headwall to toe, the average seafloor slope is about 2°. The lobes protrude 9 to 10 m above the undisturbed seafloor, indicating that the volume of displaced material, integrated over the area of the slide lobes, amounts to about $3–4 \times 10^8$ m^3.

Landslides below the Santa Barbara Channel can be lumped into two classes: the Goleta landslide complex has a headwall at shallow (100 m) depth and is by far the largest accumulation of mass-wasted debris in the channel. The other landslide class includes small failures that have headwalls under deeper water (350–500 m) (Fig. 2). Two examples of deeper-water landslides (L1 and L2 on Fig. 2) have headwalls that underlie water about 500 m deep. The headwalls cut downward into the northeast flank of a broad, west-trending, seafloor swell that developed over a growing anticline. These landslides moved northeastward, opposite in direction to landslides making up the Goleta complex. West of this complex the headwall of deep-water landslide L4, the Gaviota mudflow (Edwards et al., 1995; Lee and Edwards, 1986; Lee et al., 1991), incised the middle part of the continental slope, under water about 400 m deep. Landslide L5 occurred under the far western part of the area as represented by Fig. 2; the headwall is about 350 m below sea level.

The Gaviota mudflow lies 8 km west of the Goleta slide, on the lower part of the basin slope. From

headwall to toe, the mudflow extends downward from water depths near 380 to 500 m (Edwards et al., 1995; Thornton, 1984, 1986; Lee and Edwards, 1986; Lee et al., 1991; Hampton et al., 1996). Edwards et al. (1995) described secondary slumping and retrogressive failure of the head scarp and estimated the total displaced volume to be about $1–2 \times 10^7$ m^3. A fissure in the seafloor extends eastward from the head scarp for about 2.7 km (Fig. 2).

Lee and Edwards (1986) conducted strength tests on core samples from the Gaviota mudflow and from nearby intact sediment. These authors showed that an earthquake with equivalent pseudo-static accelerations of 0.12 *g* could have caused the sediment to fail. Lee et al. (1991) evaluated the mobility of sediment from the Gaviota mudflow after the initial failure. They determined that the mobilized (post failure) shear strength of sediment in the Gaviota mudflow was low enough that most of the sediment would have been able to flow down the continental slope, which is inclined at about 4°. This mobilized strength, however, was too high to allow flow over the more gently inclined (1°) continental slope near the mudflow's toe.

4. Geophysical data

To investigate landslides below Santa Barbara Channel, we use multibeam bathymetric data that were collected for Monterey Bay Research Institute (MBARI) using a Simrad EM300 system operated at 30 kHz. These data are shown here as shaded-relief maps of slope gradient (Fig. 2). We integrate this bathymetric information with seismic-reflection data that range from low-resolution deep-penetration data collected by Western Geophysical Company, Inc. to several kinds of high-resolution data collected by the U.S. Geological Survey in 2002 (Table 2). An Aquapulse source, a type of sleeve exploder, was used to obtain the low-resolution data.

Table 2
Types of seismic-reflection data

Collected by	Seismic source	Fold	Streamer length (m)	Frequency range (Hz)
WG[a]	Aquapulse	46	3133	8–42
USGS	2 kJ minisparker	24	240	150–1700
USGS	Huntec boomer	1	none	500–8000
USGS	Chirp	1	none	1000–8000

[a] Western Geophysical Company, Inc.

5. Research results: stratigraphy of the Goleta landslide complex

Aquapulse seismic line WSB-29 (Figs. 3 and 8) crosses the Goleta landslide complex southwestward from the shelf break to the basin floor of the Santa Barbara Channel. Despite the low stratigraphic resolution of these data, they reveal information about the total thickness of basin strata that contain landslide deposits. Features in these seismic-reflection data that we interpret as landslide deposits have poor internal reflectivity and an irregular upper surface (Fig. 6). Reflections from the deepest landslide deposits we identified occur between horizons A (170 ka) and B (200 ka) (Fig. 6). Given the low resolution of these data, we cannot preclude the possibility that landslides older than 200 ka remain unrecognized; we propose, however, that landslides in the area of the Goleta landslide complex began at least 200 ka ago.

In high-resolution minisparker seismic-reflection data, landslides appear as poor-data zones that alternate vertically with strong parallel reflections (Fig. 7). Locally, sediment producing the parallel reflections appears to have been deposited around topographic irregularities. Repeated landslides make up a considerable thickness of the basin fill under the Goleta landslide complex.

The thickness of the shallowest landslide in Fig. 7 is difficult to estimate. The poorly reflective zone associated with the shallowest landslide represents sediment about 100 m thick. Prior et al. (1984) show that a poorly reflective zone like this underlies other landslides and attribute the zones to bedding disruption caused not only by the incorporation of in situ sediment into the landslide but also to deformation of this sediment as the slide was emplacement. Perhaps as much as 50% of the volume of a landslide can be made up of mobilized in situ material. Highly reflective rocks at the base of the landslide are missing from along part of the landslide's base (Fig. 7), showing that bedding disruption can extend tens of meters downward into the basin sediment.

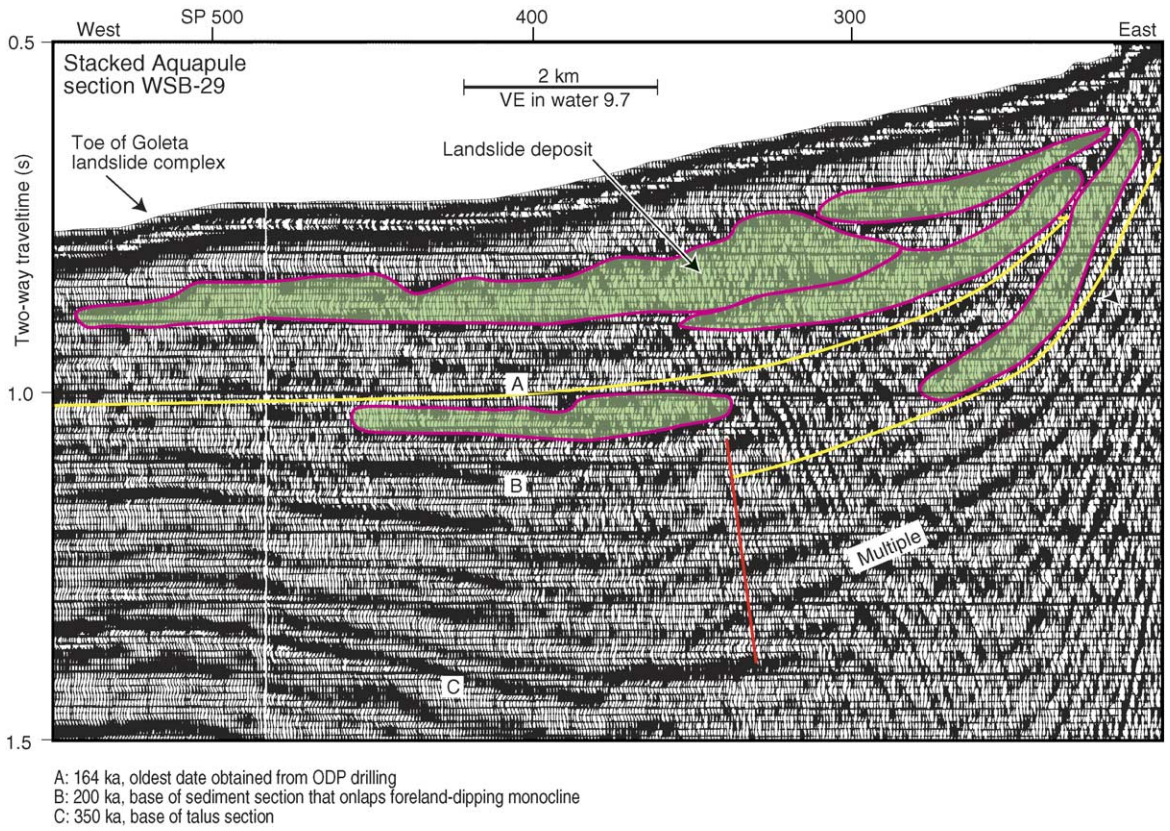

Fig. 6. Detail of Aquapulse seismic-reflection section WSB-29 obtained over the Goleta landslide complex. Location is shown in Fig. 3. The deepest buried landslides interpreted from these data, indicated with green shading, overlie reflection "B". The blue line labeled "Multiple" indicates the seafloor multiple. Table 2 shows the approximate ages of reflective horizons.

The toe of the northwest landslide lobe is about 10 m high where it curves downward to meet the seafloor (Fig. 7). Multibeam bathymetry (Fig. 2) shows that the toes of the northwest and southeast lobes of the Goleta landslide complex have similar relief above the seafloor, but the middle lobe merges smoothly with the seafloor.

6. Structural controls on the geographic extent of landslide development

6.1. Possible mass wasting east of the Goleta landslide

The part of the Goleta landslide complex that is evident in multibeam bathymetric data is restricted in occurrence to a 10-km-long section of the shelf edge and continental slope south of Coal Oil Point (Fig. 2). An important constraint for analyzing tsunami hazards concerns whether or not large landslides have occurred elsewhere along this shelf edge and whether they might recur.

One clue to where landslides have concentrated along the shelf edge is the close spatial correlation between landslides and deep anticlines. For example, the headwall of the Goleta landslide complex is spatially associated with anticlines A1, A2, and A3 (Fig. 5), and the Gaviota mudslide directly overlies anticline A4. Isolated landslide L5 in the far western part of the basin is associated with anticline A6. Although the two small landslides L1 and L2 lie along the upthrown side of the Oak Ridge fault, these landslides also conform to the association between anticlines and landslides because shallow rocks and sediment along the fault are anticlinally deformed.

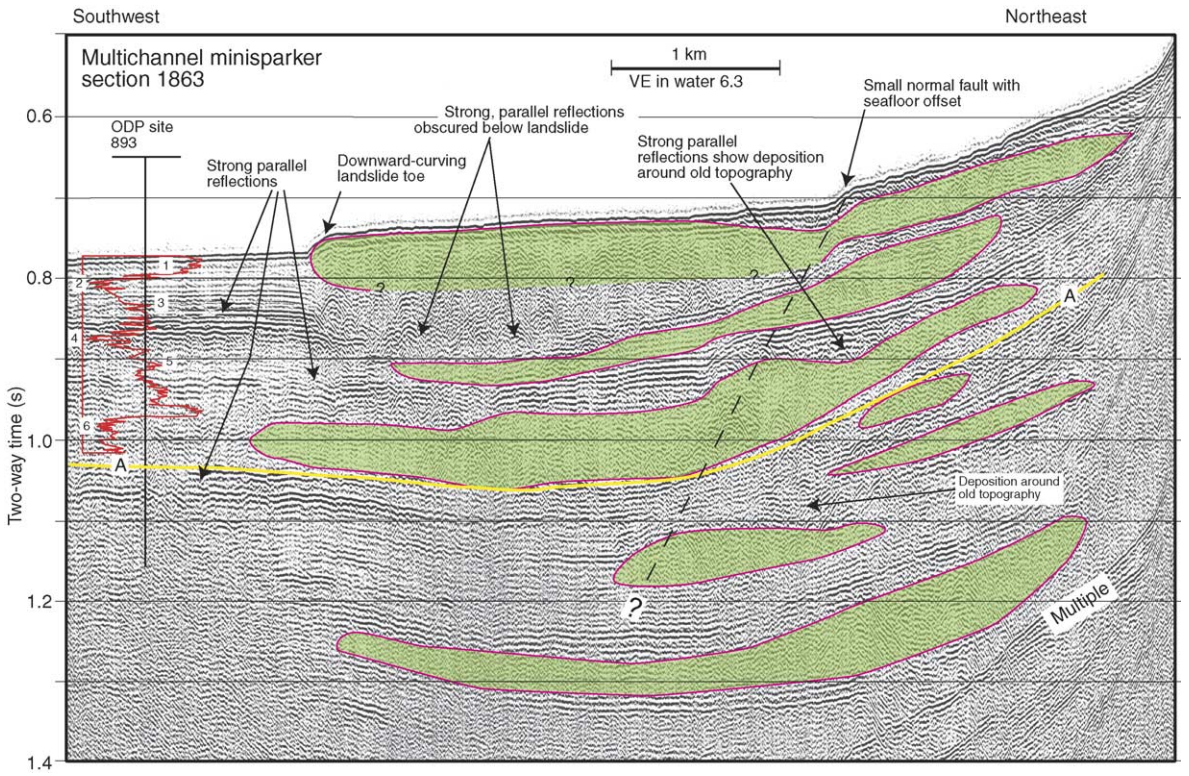

Fig. 7. High-resolution minisparker seismic-reflection data show a thick section of landslide deposits, shown with green shading, preserved beneath the Goleta landslide complex. Section location is shown in Fig. 2. The red curve shows the oxygen-isotope variation in sediment obtained from ODP site 893; numbers along this curve show marine isotope stages (Kennett, 1995). Horizon A, the yellow line, is from rocks about 160 ka old.

The Pitas Point and Oak Ridge Faults gradually converge westward below the eastern Santa Barbara Channel (Fig. 5), and below the Goleta landslide complex, these faults abruptly diverge and the Oak Ridge dies out. Where the Oak Ridge ends an anticline developed along this fault underlies the lower continental slope (left side of Fig. 8A). Comparison of seismic-reflection section 1860 (Fig. 8A) with section 1863 (Fig. 6) shows that the lower-slope anticline dies out to the west, to where the Goleta complex attains its strongest expression. We propose that the abrupt end of this anticline and the neighboring termination of the Oak Ridge Fault signals that displacement along the Oak Ridge fault and structural shortening that formed the lower-slope anticline were transferred upslope to structures associated with the North Channel–Pitas Point–Red Mountain fault system. This local displacement transfer could explain not only the Goleta landslide's position along the shelf edge but also the restricted development of large landslides along the shelf edge.

A important question to resolve to understand the possible hazard from landslide-generated tsunamis is whether mass failure will occur east of the Goleta landslide, because landslides farther east will occur closer to the city of Santa Barbara (Fig. 1). Seismic-reflection and multibeam bathymetric data show the geology along the east flank of the Goleta landslide complex (Fig. 10A and B). A seafloor groove extends eastward from the complex. Seismic-reflection data, however, show that the groove does not mark an incipient landslide because the groove shows where a fault emerges at the seafloor (Fig. 8C). Upslope from the seafloor groove, the seafloor bulges upward (Fig. 8A). This bulge is underlain by deep anticline A1 (Fig. 5), and the bulge is evidence for very young

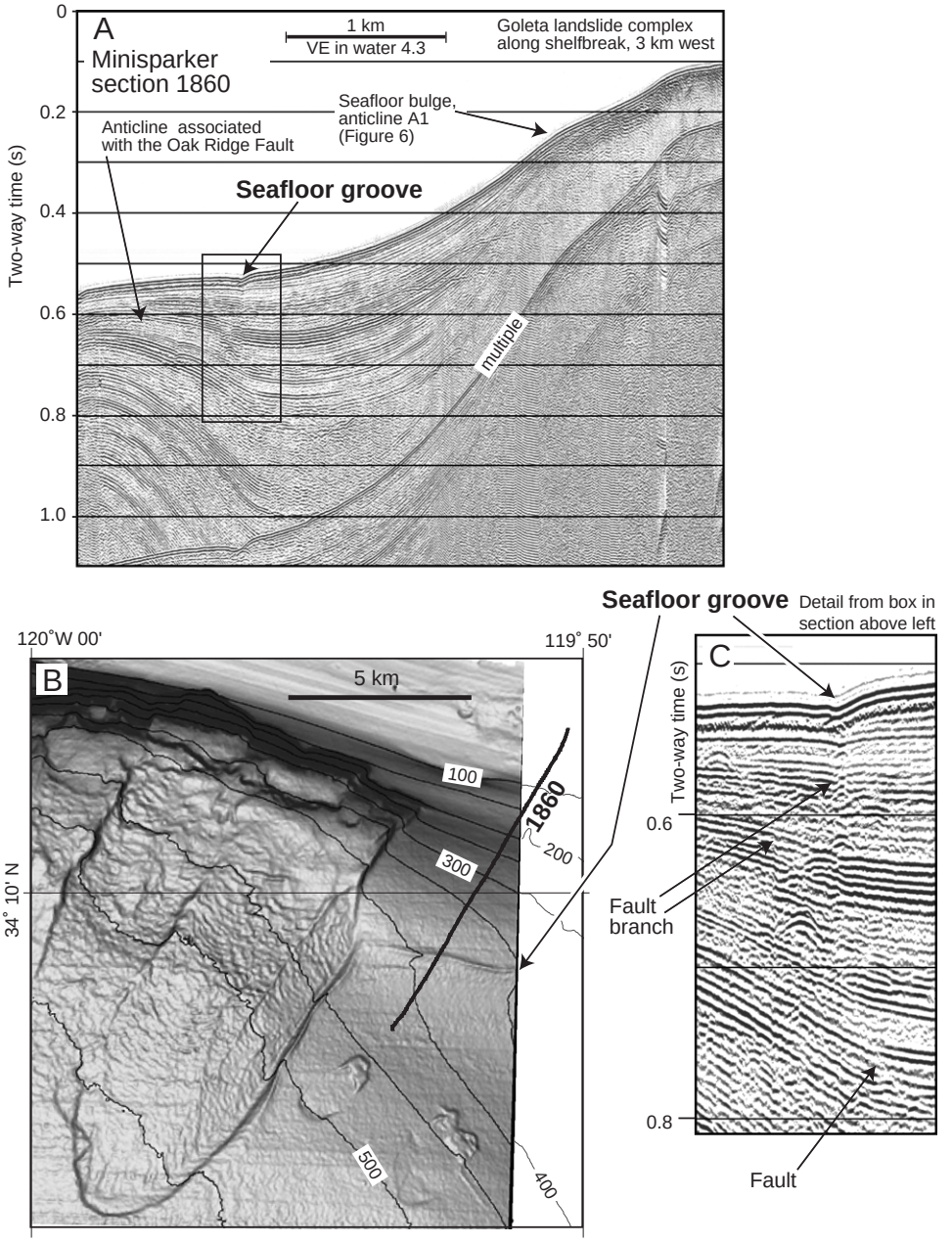

Fig. 8. (A) Seismic-reflection data showing the geologic structure along the east side of the Goleta landslide complex. (B) Multibeam bathymetric map of the Goleta landslide complex and location of the seismic section in A. (C) Expanded view of seismic-reflection data within the box shown in A. The seafloor groove evident in multibeam bathymetry and seismic-reflection data formed along a fault branch.

growth of this structure. Seismic-reflection data (Fig. 8A) show sediment under the slope is mainly well stratified; these data do not reveal the presence of buried landslides with the appearance of the ones we described above in discussing Figs. 8 and 9. Hence, although the seafloor groove does not indicate an incipient landslide, anticlinal growth may destabilize sediment under the upper slope.

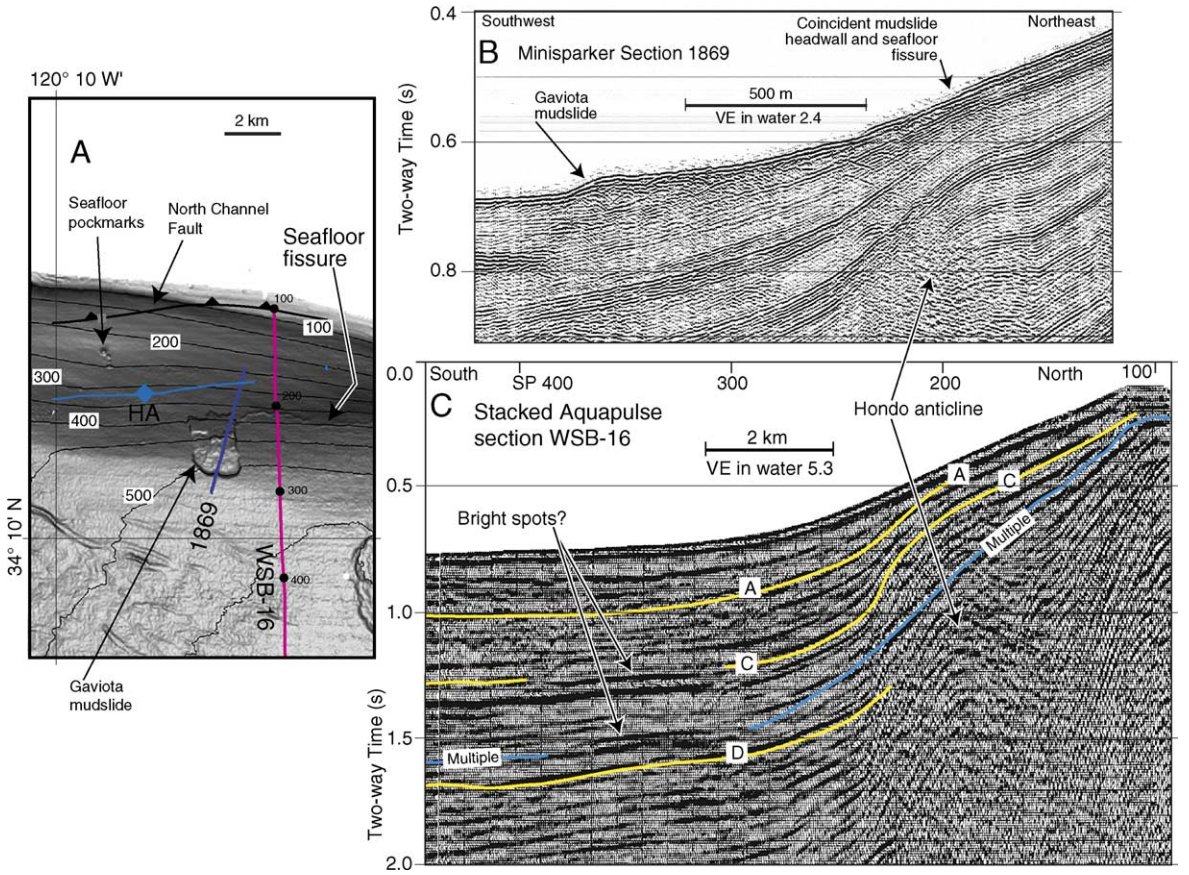

Fig. 9. (A) Multibeam bathymetric map of the area around the Gaviota mudslide. The Hondo anticline (HA) and North Channel Fault are shown. (B) High-resolution seismic-reflection section across the Gaviota mudslide and the Hondo anticline. Sediment just under the seafloor arch and thin over the Hondo anticline. The Gaviota mudslide's headwall directly overlies the anticlinal axis. (C) Deep-penetration seismic-reflection data over the Hondo anticline shows that rocks under this part of the shelf are not as strongly deformed as are rocks near the Goleta landslide complex.

6.2. Possible mass wasting west of the Goleta landslide

Multibeam bathymetry and high-resolution seismic-reflection data show the Gaviota mudslide and a fissure that extends eastward from this slide's headwall for several kilometers (Fig. 11A and B). The fissure indicates a heightened potential for additional mass wasting along the western part of the continental slope. This fissure appears analogous to fissures described from near a submarine landslide that occurred off Papua New Guinea (Tappin et al., 2001, 2002). Seismic-reflection data, however, show that the Gaviota mudslide involves only the shallowest slope sediment, and the question remains whether or not high-volume mass wasting is likely to occur there. Aquapulse seismic-reflection sections collected west of the Goleta landslide complex do not reveal buried landslide deposits like those under this complex. This is borne out by comparing Aquapulse seismic section WSB-29 (Fig. 6), across the Goleta landslide, with section WSB-16 (Fig. 11A and C), which crosses the continental slope just east of the Gaviota mudslide. Shallow rocks and sediment (above 0.8 s on Fig. 9C) under the shelf edge overlie the Hondo anticline; these materials are not as strongly deformed as are those below the headwall of the Goleta complex (Fig. 3).

We interpret the above observations to mean that the development of deep-seated submarine landslides

has been restricted to the area of the Goleta landslide complex. East of this landslide complex, anticlinal growth under the upper slope could promote mass wasting. West of this complex, growth of deep-seated landslides seems to be inhibited by a decrease in the intensity of structural development below the shelf edge. In the west, a fissure indicates where future thin sediment failures, like the Gaviota mudslide, might develop that will involve primarily the uppermost slope sediment.

7. Discussion

7.1. Emplacement age of the Goleta landslide complex

We have shown that some buried landslides are at least as old as 200 ka, but how young are the landslides directly under the seafloor? Seismic-reflection data and high resolution stratigraphy are adequate to make accurate estimates for the emplacement age of two of the landslide lobes because the landslide toe lies only 1 km away from ODP Site 893 (Shore-Based-Scientific-Party, 1994).Very high-resolution, chirp seismic-reflection data provide a firm age for the middle lobe. The toe of the middle lobe tapers gradually southwest to a sharp tip within basin sediment (Fig. 12C and D). We correlate this tip with sediment penetrated at the nearby ODP site to show that the landslide is 10 ka old (Fig. 12B and C). This date is based on reservoir-corrected C14 dates from planktic foraminifera (Kennett, 1995).

An age estimate for the northwest landslide lobe can be based on the thickness and appearance in seismic-reflection data of sediment that blankets this lobe. Sediment penetrated in the shallowest part of ODP drill site 893 appears to be well bedded in both chirp seismic-reflection data (Fig. 10E) and in very high resolution Huntec minisparker data (Fig. 4A). Well-bedded sediment at the drill site is as old as about 6 ka. If the thin blanket of well bedded sediment is the same age as at the drill site, then the northwest lobe is somewhat younger than 6 ka old.

A better age estimate for the northwest landslide lobe comes from a seismic-reflection section that shows a landslide tongue within shallow basin sediment (Fig. 13A and B). Finely layered sediment makes up much of the basin fill that underlies the seafloor, as shown along the left side of Fig. 11B. A tongue of poorly reflective sediment extends beyond the landslide toe. The well-bedded sediment probably has low shear strength and is not likely to have retained its bedding, if the landslide tongue was injected into the basin fill. Instead, the tongue's base most likely was the seafloor at the time the landslide lobe and the sediment tongue were deposited. The heavy line labeled "A" indicates that the landslide is about 8 ka old (Fig. 13B and C). We prefer this date for the northwest landslide lobe.

The southeast landslide lobe is the most difficult of the three lobes to date because none of our seismic-reflection lines cross from undisturbed basin fill to this lobe. Huntec seismic-reflection data obtained over the middle and upper parts of this lobe (Fig. 12A) reveal that the shallowest sediment has the same acoustic-facies character as sediment that blankets the northwest lobe (Fig. 10E). We favor the possibility that the main part of the southeast lobe was emplaced about 6 ka ago, which is the approximate time when finely layered sediment began to be deposited on the northwest lobe (Fig. 10B).

A largely undeformed slope apron blankets the upper part of the entire landslide complex (Fig. 12B). The northwest and southeast lobes must have been emplaced before this apron was deposited. The rate of deposition for apron sediment is difficult to estimate because the apron lies directly below the source area for the landslides, and apron deposition could have occurred at a high rate that is atypical of other areas. The parallel reflections, however, suggest little contribution to the apron from continued mass wasting.

7.2. Estimated age of deep-water landslides

Edwards et al. (1995) cite evidence that the Gaviota mudslide dates from about 300 yr. ago, and other deep-water slides appear to have developed very recently. The headwalls of the deep-water landslides occur within a narrow range of water depth (350–500 m), and all these headwalls are sharply expressed in seismic-reflection data (e.g. Fig. 9B). Furthermore, the seafloor fissure that leads east from the headwall

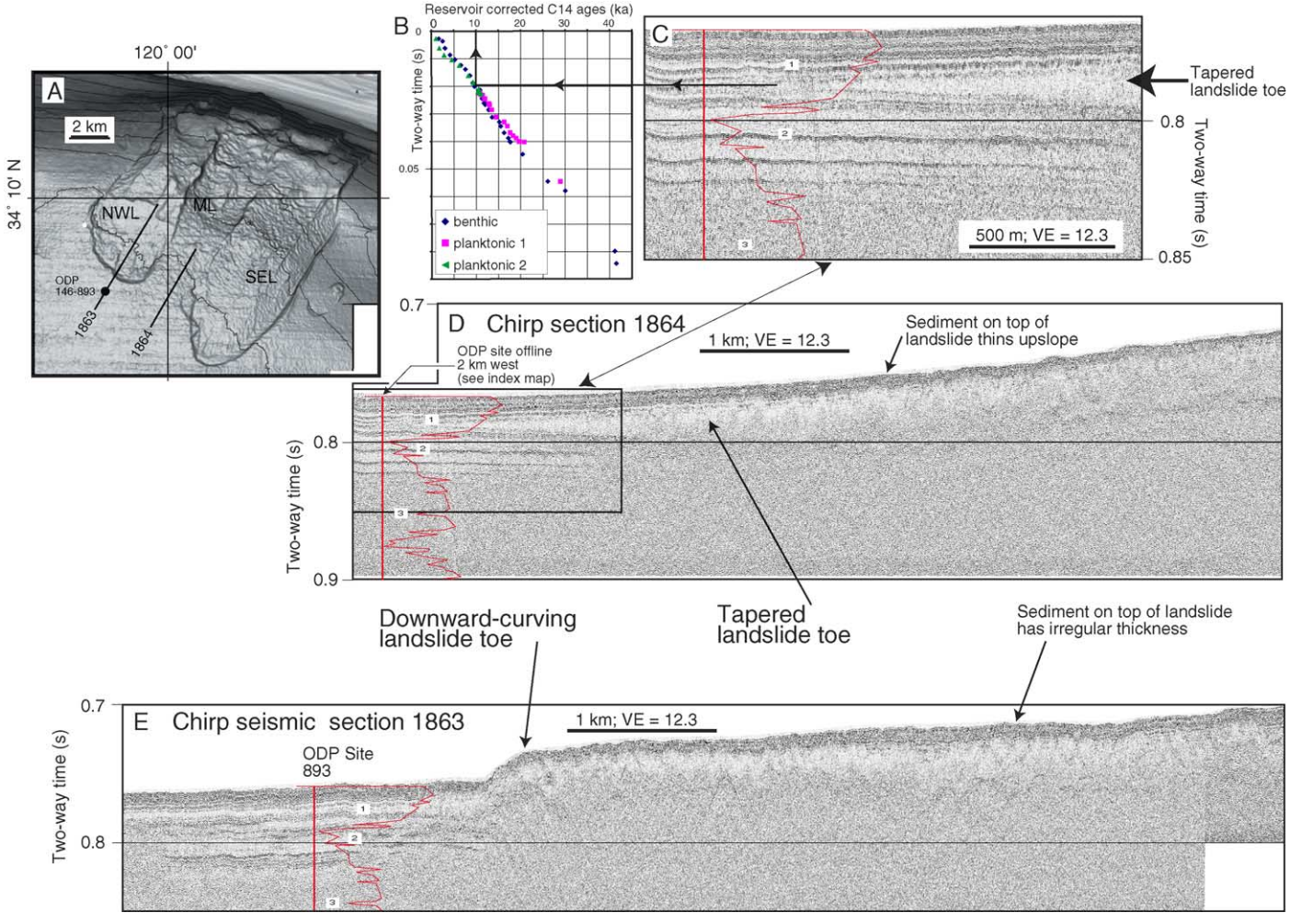

Fig. 10. (A) Multibeam bathymetric map showing tracklines for chirp seismic sections 1863 and 1864 and the three lobes of the Goleta landslide complex. NWL is northwest lobe; ML is middle lobe; SEL is southeast lobe. (B) Chronostratigraphic data from ODP Site 893 (Kennett, 1995). (C) Detail of the tapered toe of the middle landslide lobe. The red curve shows the oxygen-isotope variation in sediment drilled at the ODP site. Numbers in white boxes show oxygen-isotope stages. (D) Chirp seismic-reflection section 1864 over the middle lobe of the Goleta landslide complex. The red curve and numbers in white boxes are as in Fig. 4. The box shows the location of C. (E) Chirp seismic-reflection section 1863 over the northwest lobe of the Goleta landslide complex.

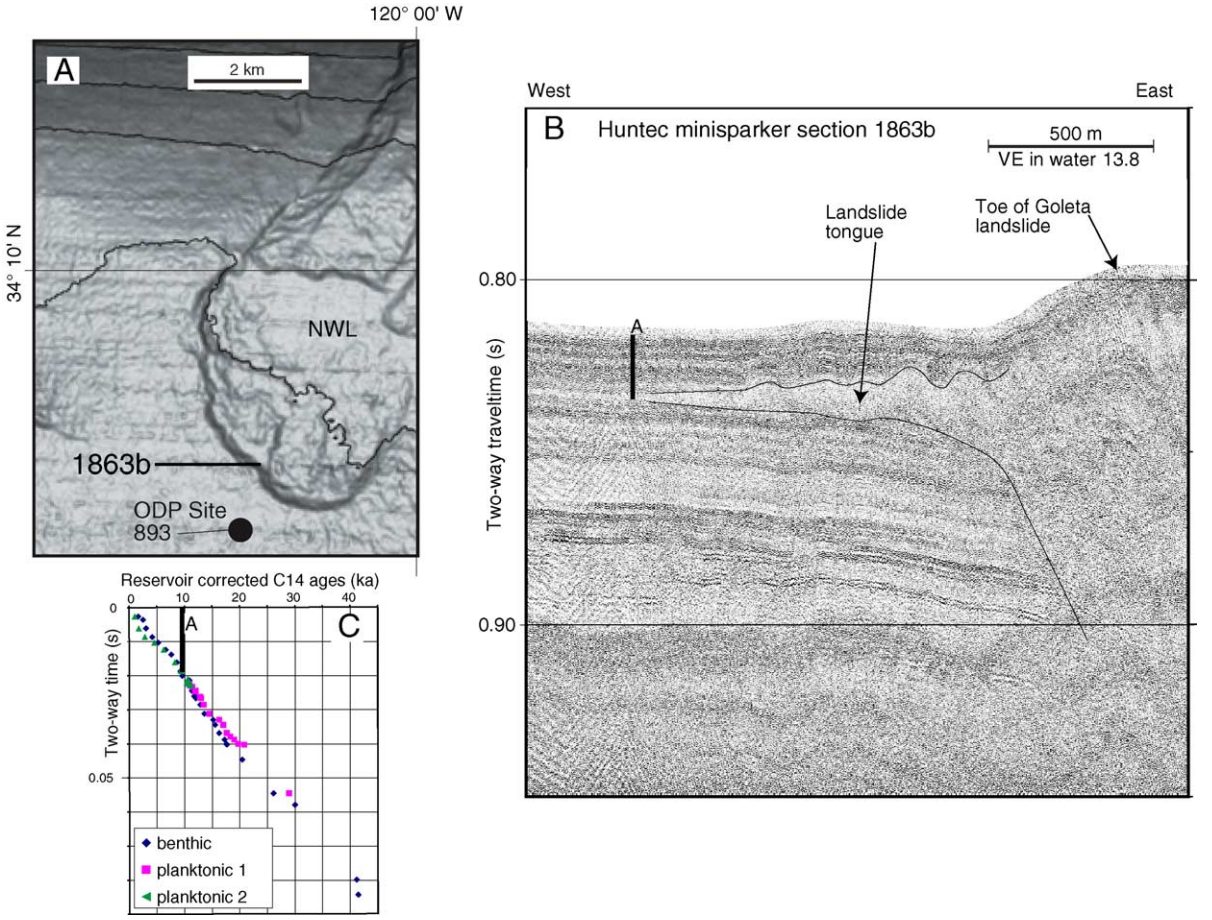

Fig. 11. (A) Multibeam bathymetric map showing the northwest lobe (NWL) of the Goleta landslide complex and the trackline for Huntec minisparker section 1863b. (B) Detail of the toe of NWL of the Goleta complex. The lower solid line indicates basin sediment affected by emplacement of the landslide. The heavy solid line labeled "A" spans the travel time interval to the base of the disrupted sediment, which was probably the seafloor when the slide was emplaced. (C) Chronostratigraphic data from ODP Site 893. The heavy solid line labeled "A" shows that the landslide is about 10 ka old.

of the Gaviota mudslide (Figs. 2 and 11A) has not been smoothed by recent sediment deposition. For these reasons, the deep-water landslides are likely to be quite young.

7.3. Sediment source for the Goleta landslide complex

Multibeam bathymetric data reveal the source area for sediment now contained within the Goleta landslide complex. The headwall of the complex indents into an area of the shelf where the seafloor is smooth, whereas east and west of the headwall, the seafloor over the continental shelf is rough (Fig. 13A). The rough seafloor is probably caused by the outcropping of Pliocene and older bedrock. In support of this contention, the north end of seismic line 1864 (Fig. 13B) shows that under the shelf, southwest-dipping rocks of probable Miocene and Pliocene age are truncated by an erosional unconformity at or near the seafloor. This section also reveals that under the shelf edge an angular unconformity separates the dipping rocks from overlying beds that dip less steeply southwest. We propose that this unconformity separates late Quaternary sediment in a shelf-edge delta, above, from underlying bedrock. The down-dip ends of some deltaic strata end at the

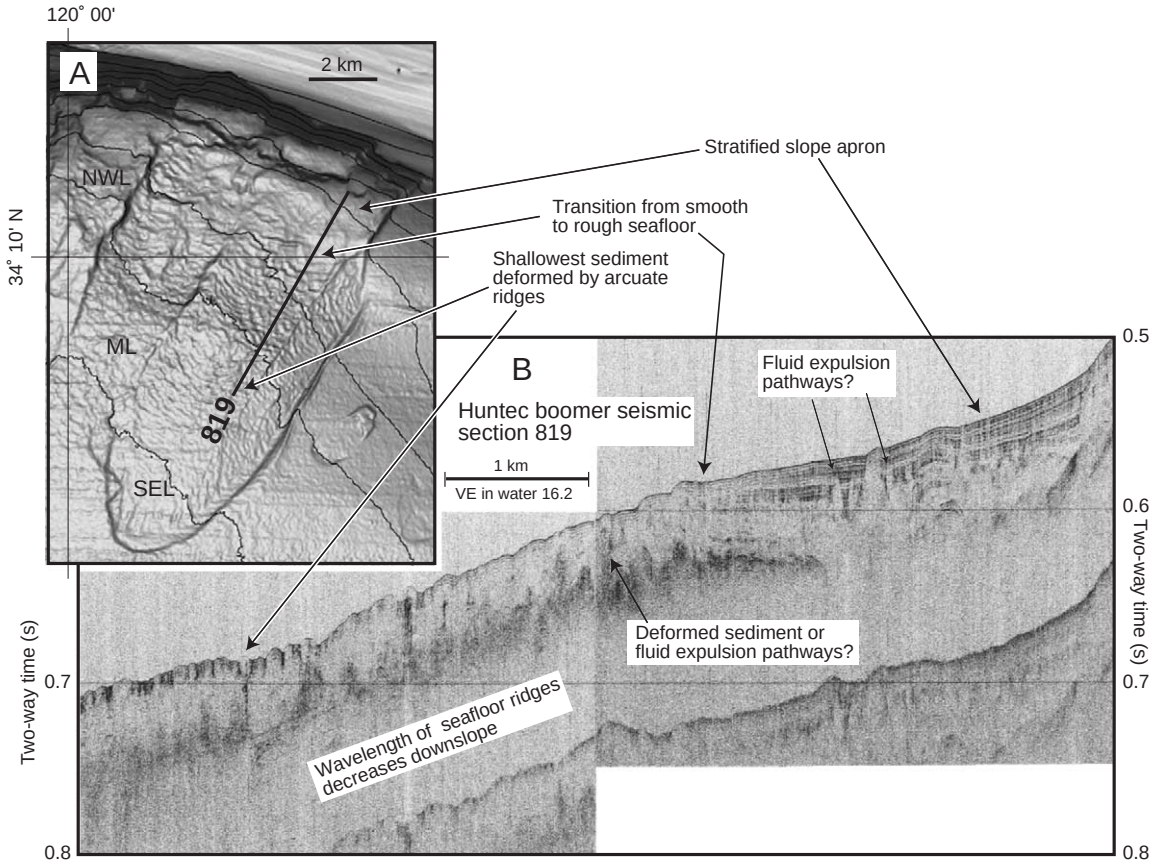

Fig. 12. (A) Multibeam bathymetric map showing the southeast lobe of the Goleta landslide complex and the location of Huntec seismic section 819 over the middle and upper part of this lobe. NWL is northwest landslide lobe; ML is middle lobe; SEL is southeast lobe. (B) Very high resolution Huntec seismic section 819 showing that the shallowest sediment layers over the lower part of the landslide lobe are deformed into seafloor ridges. Some features in an otherwise undeformed sediment apron in the upper part of the lobe may have been caused by fluid expulsion.

seafloor (Fig. 13B). The original southwestward continuations of these strata are now part of the landslide complex. The delta is relatively thin (50 m) in the west (Fig. 13A), but a thicker (100 m) deltaic section remains perched under the middle part of the shelf edge shown in Fig. 13A. Apparently, remnants of the shelf-edge delta sediment could be dislodged to cause a tsunami.

Along the base of the headwall of the Goleta landslide complex, a discontinuous ridge parallels the shelf edge (Fig. 13A). This ridge is made up of sediment bodies, locally with coherent bedding, as on seismic section 1864 (Fig. 13B). These bodies are rotational slump blocks that likely slid down from the shelf-edge delta.

7.4. Factors promoting landslides

The close connection between submarine landslides and active tectonics has been emphasized previously (e.g. Tappin et al., 2001, 2002; von Heune et al., 2004). In the case of landslides in the Santa Barbara Channel, one long-term tectonic process is the growth of geologic structures under the northern shelf edge. We focus on the North Channel and Pitas Point Faults and the anticlines arrayed along these faults (Fig. 5). Interpretive differences about these faults indicate either that they are separate (Heck, 1998 and Fig. 5) or that they form one continuous fault (Sorlien et al., 2000). Our data do not clarify this issue.

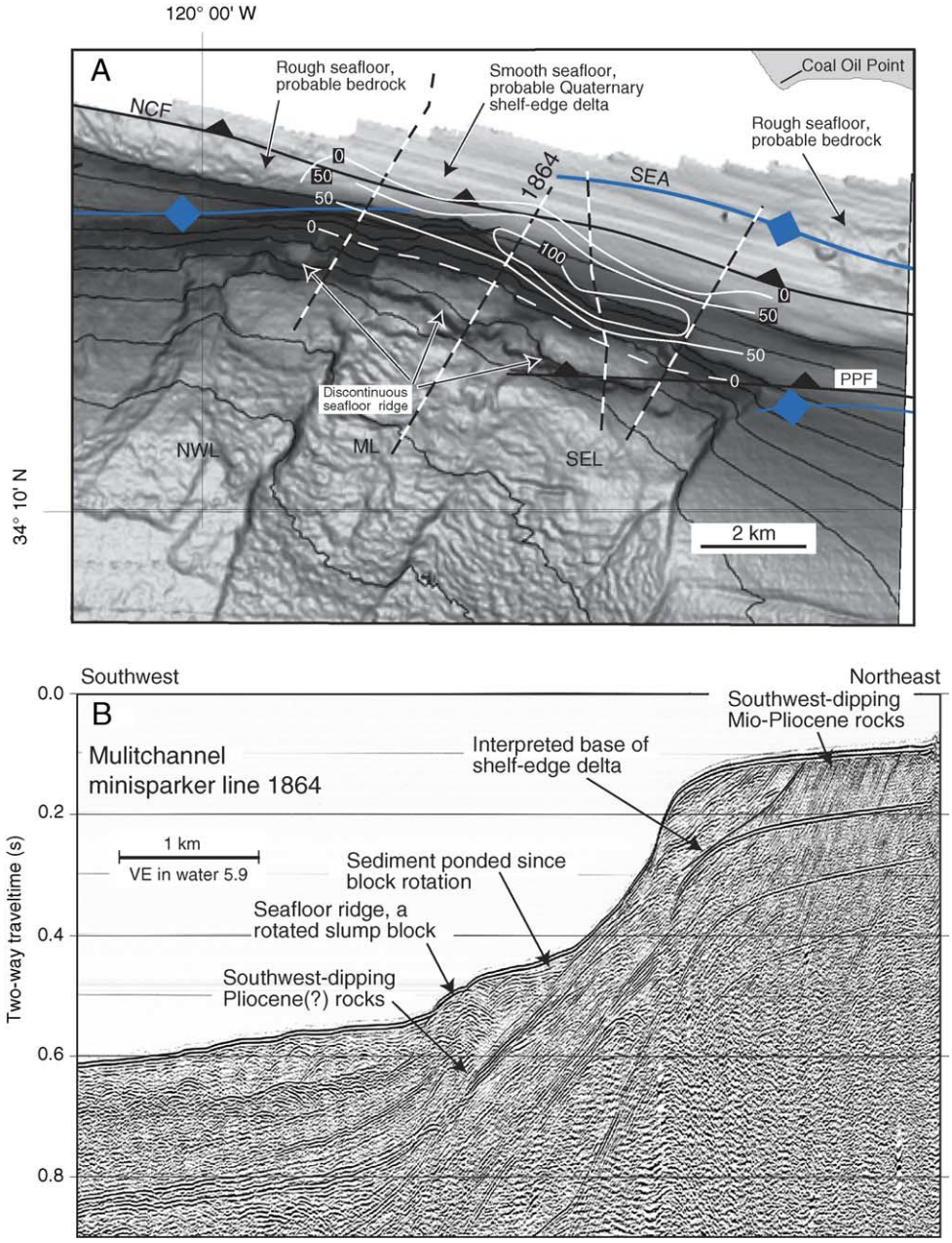

Fig. 13. (A) Multibeam bathymetric map showing tracklines for multichannel minisparker lines 1863 through 1866 that cross the headwall of the Goleta landslide complex. White contour lines (dashed where inferred) show the thickness in meters of the interpreted shelf-edge delta that supplied material to the landslide. NWL is northwest landslide lobe; ML is middle lobe; SEL is southeast lobe. NCF is North Channel Fault; PPF is Pitas Point Fault; SEA is South Elwood anticline. Fault and anticline locations are from Heck (1998). (B) Multichannel minisparker line 1864 over the middle part of the headwall. The interpreted shelf edge delta of probable late Quaternary age overlies older rocks with angular unconformity.

Miocene and Pliocene rocks below the shelf edge near the Goleta landslide are complexly deformed, and one hypothesis to explain this deformation is that these rocks have been deformed along north-dipping thrust faults to form a passive-roof duplex structure (Edwards and Heck, 1998). Other structural models can explain the configuration of rocks under the shelf edge, but the result is the same, namely, that the less competent rocks rotate to dip in the direction of thrust movement, and a foreland-dipping monocline develops.

Near the Goleta landslide, rocks making up the proposed foreland-dipping monocline are thought to include mainly Sisquoc Formation and younger rocks (Edwards and Heck, 1998). Seismic-reflection data obtained over this landslide complex reveal what may be the southwest-dipping rocks in a foreland-dipping monocline (Fig. 3), but our data lack resolution to show an underlying duplex structure. As the duplex structure develops, it progressively steepens the basinward dip of rocks within and sediment deposited on top of the foreland-dipping monocline. This steepening would tend increase the potential for mass wasting.

The Santa Barbara Basin is a major petroleum province, and a vigorous hydrologic regime probably characterizes this basin. For this reason, analyses dealing with how submarine landslides are triggered below the Santa Barbara Channel need to include the possible effects of fluid flux on sediment stability. Probable bright spots in seismic-reflection data (Fig. 9C) indicate the likely entrapment of hydrocarbon gasses. Other geophysical evidence for the flow of aqueous or hydrocarbon fluids include pockmarks at the seafloor (Fig. 9A) and possible fluidization features (Fig. 12B). The fluidization features interrupt strata forming an upper-slope apron that was deposited across the width of the upper Goleta landslide complex, presumably after the last major landslide movement occurred. Fluid flowing through the headwall area of a landslide might initiate further mass wasting. In particular, a fluid-pressure pulse that accompanied an earthquake on the major fault system that underlies the landslide could unleash further landsliding.

Earthquakes are a likely trigger for landslides under Santa Barbara Channel. Historical earthquakes having magnitudes ≥ 5 occur about every ~20 yrs, particularly in the area east of the main landslide concentration (Fig. 1).

7.5. Tsunamis caused by landslide movement

Historical accounts suggest that a tsunami from the 1812 Santa Barbara earthquake had a runup height of 2–4 m (Borrero et al., 2001; NOAA, 2003; Pararas-Carayannis, 2004). Animations available on the internet illustrate how tsunamis generated by a landslide south of the Channel Islands and by an earthquake that ruptured the Channel Islands thrust fault would propagate throughout the Santa Barbara Channel (USC Tsunami Research and Group, 2004). This thrust fault is proposed to be the through-going master blind fault, located 5 to 15 km below the Santa Barbara Channel, into which all shallower faults merge (Shaw et al., 1994). Numerical modeling indicates that an M7 earthquake along this fault might produce a 2-m tsunami runup along the entire north shore of the Santa Barbara Channel west of Ventura (Borrero et al., 2001).

Numerical modeling of tsunamis in Santa Barbara Channel indicates a moderate threat (Borrero et al., 2001). For the case of a small-volume (0.2 km^3) slope failure like the Gaviota mudslide, the runup height could be about 2 m (Borrero et al., 2001); whereas a larger-volume (4 km^3) failure might cause a tsunami runup height as large as 20 m. These landslide-generated tsunami waves, however, would affect a much smaller length (10 km) of the shore than would tsunamis caused by earthquakes.

Ward (2001) analyzed tsunamis resulting from submarine landslides that ranged from a simple block slide to slides having more complex runouts and detachment styles. Given these styles of sliding, the tsunami's height is controlled by three main factors: water depth, landslide speed, and landslide volume. If the horizontal dimensions of the slide are greater than approximately three times the water depth, then increasing the water depth above the slide will increase the attendant tsunami runup. For smaller landslides, increasing the water depth will result not only in wave attenuation for wave propagating toward deep-water, because of the inefficiency of displacing the entire water-column, but also in wave amplification for wave propagating toward shallow water, because shoaling water causes waves to increase in

height. Water depth around the Goleta landslide complex is known very well from multibeam bathymetry. Because the dimensions of the three main lobes of the Goleta landslide complex are greater than three times the water depth, movement of the slide in deep-water would accentuate southward propagating waves.

The second factor controlling tsunami height is landslide volume—larger volume leads to greater wave heights. Seismic-reflection data show the volume of the shelf-edge delta that remains in place above the Goleta landslide complex (Fig. 13). Future tsunami-hazard assessment could proceed on the assumption that all or part of this remaining volume would fail.

The third factor is landslide speed. For a simple sliding-block model, the optimum landslide velocity for generating tsunamis equals the phase velocity of the tsunami waves. Water depths near the Goleta landslide complex yield optimum landslide speeds having high values between 30 and 125 m/s.

In our opinion, debris making up the Goleta landslide lobes moved much more slowly downslope than the optimum speeds cited above. This is based on drilling results from ODP Site 893, which show that in sediment younger than 60 ka, brief oxic and anoxic oceanographic events in the Santa Barbara Channel correlate closely in time with excursions in oxygen-isotope values found in Greenland ice cores (Behl and Kennett, 1996). The ODP sediment apparently retains records of fleeting Dansgaard–Oeschger climatic events. It is surprising to us that this fine-scale climatic record was not disrupted by emplacement of the nearby Goleta landslide complex. At the seafloor, the toe of this complex halted only 1 km from the drill site, and some subsurface landslide tongues approach even closer to the site. Seemingly, a fast moving landslide would cause turbid flow that would be widely dispersed. If such sediment dispersal occurred repeatedly since 60 ka ago, it is not evident from the detailed climate record from the ODP site.

8. Conclusion

Landslides under Santa Barbara Channel began to occur at least 200 ka ago; however, the most recent ones making up the Goleta landslide complex appear to be primarily early Holocene (8–10 ka). Quaternary deltaic sediment clings to the shelf edge directly above the headwall of the main Goleta landslide complex, and future landslides involving material in this delta are possible. Future landslides are most likely to develop from material contained in the thick eastern part of the delta. Although major earthquakes are the most obvious landslide triggers, landslide initiation does not appear to be exclusively dependent on seismicity, because other processes, such as subsurface fluid flow, the rate of sediment accumulation in the shelf-edge delta, and the destabilizing influence of structural growth, could combine to unleash landslides. Future tsunami modeling will benefit from contour maps of delta thickness based on data presented here and on estimates of landslide susceptibility.

Acknowledgements

We thank Eric L. Geist and Kevin M. Schmidt of the U.S. Geological Survey and two anonymous reviewers for comments that greatly improved this report.

References

Atwater, T.M., 1970. Implications of plate tectonics for the Cenozoic evolution of western North America. Geol. Soc. Amer. Bull. 81, 3513–3536.

Behl, R.J., Kennett, J.P., 1996. Brief interstadial events in the Santa Barbara Basin, NE Pacific, during past 60 kyr. Nature 379, 243–246.

Borrero, J.C., Dolan, J.F., Synolakis, C.E., 2001. Tsunamis within the eastern Santa Barbara Channel. Geophys. Res. Lett. 28 (4), 643–646.

Burdick, D.J., Richmond, W.C., 1982. A summary of geologic hazards for proposed OCS oil and gas lease sale 68, southern California. Open-file rep. U. S. Geol. Surv. 82-0033 (41 pp.).

Corbett, E.J., Johnson, C.E., 1982. The Santa Barbara, California, earthquake of 13 August 1978. Bull. Seismol. Soc. Am. 72, 2201–2226.

Duncan, J.R., Hoover, R.A., Pflum, C.A., Widmier, J.M., Daetwyler, C.C., 1971. Near surface geology of the Santa Ynez Unit, Santa Barbara Channel, California. Esso Production Research Company Report. 58 pp.

Edwards, E.B., Heck, R.G., 1998. Gato Canyon field, Santa Barbara Channel, California. Structure and petroleum geology, Santa Barbara channel, Miscellaneous Publication, vol. 46. Pacific Section American Association Petroleum Geologists and Coast Geological Society, Bakersfield, CA, pp. 293–300.

Edwards, B.D., Lee, H.J., Field, M.E., 1995. Mudflow generated by retrogressive slope failure, Santa Barbara Basin California. J. Sediment. Res., Sect. A Sediment. Pet. Proc. 65, 57–68.

Eichhubl, P., Greene, H.G., Maher, N., 2002. Physiography of an active transpressive margin basin; high-resolution bathymetry of the Santa Barbara Basin, southern California continental borderland. Mar. Geol. 184, 95–120.

Elliott, W., Kamerling, M.J., 1995. Seismic hazards in the Santa Barbara Channel using high resolution seismic reflection data and dated horizons from ODP 893. Eos Trans. AGU 76 (46), 417.

Ellsworth, W.L., 1990. Earthquake history, 1769–1989. U.S. Geol. Surv. Prof. Pap. 1515, 153–187.

Engebretson, D.C., Cox, A., Gordon, R.G., 1985. Relative motions between oceanic and continental plates in the Pacific basin. Geological Society of America Special Paper, vol. 206. 59 pp.

Evernden, J.F., Thompson, J.M., 1985. Predicting seismic intensities. In: Ziony, J.I. (Ed.), Evaluating Earthquake Hazards in the Los Angeles Region — an Earth-Science Perspective, U.S. Geological Survey Professional Paper, vol. 1360, pp. 151–202.

Grauzinis, V.J., Joy, J.W., Putz, R.R., 1965. The Reported California Tsunami of December 1812. Environmental Impact Report for San Onofre Nuclear Power Station. Referred to at the website http://www.crustal.ucsb.edu/ics/sb_eqs/SBEQCatlog/SBEQCATINTRO.html.

Hampton, M.A., Lee, H.J., Locat, J., 1996. Submarine landslides. Rev. Geophys. 34, 33–59.

Heck, R.G., 1998. Santa Barbara Channel regional formline map, top Monterey Formation. In: Kunitomi, D.S., Hopps, T.E., Galloway, J.M. (Eds.), Structure and petroleum geology, Santa Barbara channel, California, Miscellaneous Publication, vol. 46. Pacific Section American Association Petroleum Geologists and Coast Geological Society, Bakersfield, CA, pp. 183–184. 1 sheet.

Hornafius, J.S., Luyendyk, B.P., Terres, R.R., Kamerling, M.J., 1986. Timing and extent of Neogene tectonic rotation in the western Transverse Ranges, California. Geol. Soc. Amer. Bull. 97, 1476–1487.

Huftile, G.J., Yeats, R.S., 1995. Convergence rates across a displacement transfer zone in the western Transverse Ranges, Ventura basin, California. J. Geophys. Res. 100, 2043–2067.

Ingram, B.L., Kennett, J.P., 1995. Radiocarbon chronology and planktonic-benthic foraminiferal ^{14}C age differences in Santa Barbara Basin sediments, Hole 893A. In: Kennett, J.P., Baldauf, J.G., Lyle, M. (Eds.), Proceedings of the Ocean Drilling Program, Scientific Results, vol. 146 (Pt. 2), pp. 19–27.

Kamerling, M.J., Luyendyk, B.P., 1985. Paleomagnetism and Neogene tectonics of the northern Channel Islands, California. J. Geophys. Res 90, 12485–12502.

Kamerling, M., Nicholson, C., 1996. The Oak Ridge fault and fold system, eastern Santa Barbara Channel, California. Southern California Earthquake Center Annual Report, vol. 11, pp. C26–C30.

Kamerling, M.J., Sorlien, C.C., Archuleta, R., Nicholson, C., 2001. Three-dimensional geometry and interactions of faults and structures along the northern margin of the Santa Barbara Channel, California. Am. Assoc. Pet. Geol. Bull 85, 1127–1128.

Kamerling, M.J., Sorlien, C., Nicholson, C., 2003. 3D development of an active oblique fault system, northern Santa Barbara Channel, California. Seismol. Res. Lett. 74, 248.

Kennett, J.P., 1995. Latest Quaternary benthic oxygen and carbon isotope stratigraphy: hole 893A, Santa Barbara Basin, California. In: Kennett, J.P., Baldauf, J.G., Lyle, M. (Eds.), Proceedings of the Ocean Drilling Program, Scientific Results, vol. 146 (Pt. 2), pp. 3–18.

Lee, H.J., Edwards, B.D., 1986. Regional method to assess offshore slope stability. J. Geotech. Eng. 112, 489–509.

Lee, W.H.K., Johnson, C.E., Henyey, T.L., Yerkes, R.L., 1978. A preliminary study of the Santa Barbara, California, earthquake of August 13, 1978, and its major aftershocks. U. S. Geological Survey Circular C, vol. 797, p. 11.

Lee, H.J., Schwab, W.C., Edwards, B.D., Kayen, R.E., 1991. Quantitative controls on submarine slope failure morphology. Mar. Geotechnol. 10, 143–158.

Martinson, D.G., et al., 1987. Age dating and the orbital theory of the ice ages: development of a high-resolution 0 to 300,000 year chronostratigraphy. Quat. Res. 27, 1–29.

McGroder, M., Millson, C., Gardner, D., 1994. Timing and geometry of left-slip faulting and compressional folding in Hondo field, western Santa Barbara Channel. Am. Assoc. Pet. Geol. Bull. 78, 670.

Nicholson, C., Sorlien, C., Atwater, T., Crowell, J.C., Luyendyk, B.P., 1994. Microplate capture, rotation of the western transverse ranges, and initiation of the San Andreas transform as a low-angle fault system. Geology 22, 491–495.

NOAA, 2003. Tsunami runup database, "http://www.ngdc.noaa.gov/seg/hazard/tsrnsrch_idb.shtml". Last accessed 12/2003.

Pararas-Carayannis, G., 2004. The Santa Barbara, California, Earthquakes and Tsunami(s) of December 1812. "http://www.drgeorgepc.com/Tsunami1812SantaBarbara.html", website last accessed 3/2004.

Prior, D.B., Bornhold, B.D., Johns, M.W., 1984. Depositional characteristics of a submarine debris flow. J. Geol. 92, 707–727.

Richmond, W.C., Cummings, L.J., Hamlin, S., Hagaty, M.E., 1981. Geologic hazards and constraints in the area of OCS oil and gas sale 48, southern California. Open-file rep. U. S. Geol. Surv. 81-307, 33.

Satake, K., Somerville, P.G., 1992. Location and size of the 1927 Lompoc, California earthquake from tsunami data. Bull. Seismol. Soc. Am. 82, 1710–1725.

Shaw, J., Hook, S.C., Suppe, J., 1994. Structural trend analysis by axial surface mapping. Am. Assoc. Pet. Geol. Bull. 78, 700–721.

Shore-Based-Scientific-Party, 1994. Site 893. In: Kennett, J.P., B.J.G. (Eds.), Proceedings Ocean Drilling Program, Initial Reports, vol. 146 (Pt. 2). College Station, TX, pp. 5–50.

Sorlien, C., Kamerling, M.J., 2000. Fault displacement and fold contraction estimated by unfolding of Quaternary strata, onshore and offshore Ventura basin. NEHRP Report 99HQGR0080. 21 pp.

Sorlien, C.C., Gratier, J.P., Luyendyk, B.P., Hornafius, J.S., Hopps, T.E., 2000. Map restoration of folded and faulted late Cenozoic strata across the Oak Ridge fault, onshore and offshore Ventura basin, California. Geol. Soc. Amer. Bull. 112, 1080–1090.

Sylvester, A.G., Brown, G.C., 1997. Neotectonics and Associated Sedimentation, Ventura Basin, California, Field Trip Guide Book. Coast Geological Society, Ventura, Ca, pp. 1–16.

Tappin, D.R., Watts, P., McMurtry, G.M., Lafoy, Y., Matsumoto, T., 2001. The Sissano, Papua New Guinea tsunami of July 1998—offshore evidence on the source mechanism. Mar. Geol. 175 (1–4), 1–23.

Tappin, D.R., Watts, P., McMurtry, G.M., Lafoy, Y., Matsumoto, T., 2002. Prediction of slump generated tsunamis: the July 17th 1998 Papua New Guinea event. Sci. Tsunami Hazards 20, 222–238.

Tennyson, M.E., Kropp, A.P., 1998. Regional Cross Section across Santa Barbara Channel from Northwestern Santa Rosa Island to Canada de Molino, Structure and Petroleum Geology, Santa Barbara Channel, California, Miscellaneous Publication, vol. 46. Pacific Section of the American Association of Petroleum Geologists and Coast Geological Society, Bakersfield, CA, pp. 185–194.

Thornton, S.E., 1984. Basin model for hemipelagic sedimentation in a tectonically active continental margin: Santa Barbara Basin, California Continental Borderland. In: Stow, D.A.V., Piper, D.J.W. (Eds.), Fine-grained sediments: deep water processes and facies, Special Publication, vol. 15. Geol. Soc. London, London, pp. 377–394.

Thornton, S.E., 1986. Origin of mass flow sedimentary structures in hemipelagic basin deposits; Santa Barbara Basin, California Borderland. Geo Mar. Lett. 6, 15–19.

Toppozada, T.R., Real, C.R., Parke, D.L., 1981. Preparation of isoseismal maps and summaries of reported effects for pre-1900 California earthquakes. California Division of Mines and Geology Open-File Report, vol. 81-11, pp. 172–174.

USC, Tsunami, Research and Group, 2004. California Tsunami Models and Animations. "http://www.usc.edu/dept/tsunamis/video/calvid/", website last accessed 12/2003.

Varnes, D.J., 1978. Slope-stability problems of Circum-Pacific region as related to mineral and energy resources. Am. Assoc. Pet. Geol. Bull. 62, 1238.

von Heune, R., Ranero, C.R., Watts, P., 2004. Tsunamigenic slope failure along the middle America trench in two tectonic settings. Mar. Geol. 203, 303–317.

Ward, S.N., 2001. Landslide tsunami. J. Geophys. Res 106, 11201–11215.

Yeats, R.S., Huftile, G.J., 1995. The Oak Ridge fault system and the 1994 Northridge earthquake. Nature 373, 418–420.

Yeats, R.S., Olson, D.J., 1984. Alternate fault model for the Santa Barbara, California, earthquake of 13 August 1978. Bull. Seismol. Soc. Am. 74, 1545–1554.

Yeats, R.S., Huftile, G.J., Grigsby, F.B., 1988. Oak Ridge fault, Ventura fold belt, and the Sisar decollement, Ventura basin, California. Geology 16, 1112–1116.

Yeats, R.S., Huftile, G.J., Stitt, L.T., 1994. Late Cenozoic tectonics of the east Ventura basin, Transverse Ranges, California. Am. Assoc. Pet. Geol. Bull. 78, 1040–1074.